or more briefly as

$$[T_{ij}][a_{jK}] = \gamma_K^2[P_{ij}][a_{jK}] \tag{45}$$

and for the Rth solution as

$$[T_{ij}][a_{jR}] = \gamma_R^2[P_{ij}][a_{jR}]. \tag{46}$$

Take the transpose of (2) to get

$$\{a_{jK}\}[T_{ji}] = \gamma_K^2\{a_{jK}\}[P_{ji}],$$

or

$$\{a_{jK}\}[T_{ij}] = \gamma_K^2\{a_{jK}\}[P_{ij}], \tag{47}$$

since $T_{ij}=T_{ji}$ and $P_{ij}=P_{ji}$ and where $\{a_{jk}\}$ is a row matrix. Postmultiply (4) by $[a_{jR}]$, premultiply (3) by $\{a_{jk}\}$, and subtract to get

$$(\gamma_K^2 - \gamma_R^2)\{a_{jK}\}[P_{ij}][a_{jR}] = 0. \tag{48}$$

When $\gamma_K^2 \neq \gamma_R^2$, (5) gives

$$\sum_{n=0}^{N}\sum_{s=0}^{N} a_{nK}a_{sR}P_{sn} = 0,$$

upon development of the matrix product. This proves the orthogonality of the eigenvectors.

Coupling Through an Aperture Containing an Anisotropic Ferrite*

DONALD C. STINSON†

Summary—**Coupling through an aperture containing anisotropic ferrites is investigated theoretically by a simple extension of Bethe's small-hole coupling theory to include the dipole moment of the body in the aperture. The magnetic dipole moment of the ferrite body is ordinarily a vector but becomes a tensor upon the application of a magnetostatic field. This new theory is applicable to any situation where Bethe's small-hole coupling theory is valid. Experimental verification was quite satisfactory and was obtained on two Bethe-hole type couplers: one with the waveguides parallel, and the other with the waveguides perpendicular.**

Introduction

THE THEORY of coupling through small windows was formulated by Bethe more than a decade ago.[1] Initially, he found that the amplitudes of the modes excited in a waveguide by a window were proportional to

$$\int \overline{E}_1 \times \overline{H}_2 \cdot \bar{n} ds$$

where field 1 is the excited field, field 2 is a normal mode of the guide, and $\bar{n}$ is the inward normal. Later, he evaluated the integral over the window by developing a lumped-constant theory[2] for small windows and then applied this lumped-constant theory to side windows[3] in waveguides.

Bethe's coupling theory depends upon his lumped-constant theory for small windows, which in turn depends upon replacing the excitation caused by the window by a quantity which is proportional to the following parameters: 1) frequency; 2) the normal electric or tangential magnetic field (exciting field) which would exist at the center of gravity of the window if the window were replaced by a solid metal wall; 3) the corresponding fields (induced fields) of the normal modes which are excited by the window; and 4) lumped constants (polarizabilities) which are functions only of the shape and dimensions of the window. The basis of his lumped-constant theory depends upon the fact that the excitation of the window can be replaced by "equivalent" electric and magnetic dipole moments. These "equivalent" electric and magnetic dipole moments lead him to consider the polarizabilities (which are defined as the "equivalent" dipole moments per unit incident field) as the true lumped constants of the window. This is logical since a window may act as either an inductive or capacitive element, depending upon its location and the propagating mode in the waveguide.

Since his coupling theory applies only to cases where the window and the waveguides are filled with the same isotropic and homogeneous material, it is the purpose of this paper to extend his theory to include cases where the window is completely filled with an anisotropic ferrite. The ferrite involved is anisotropic in the sense that its permeability becomes a tensor upon the application of a magnetostatic field. This extension will be made by adding the "equivalent" magnetic dipole moment of the ferrite to that of the window.

* Manuscript received by the PGMTT, November 7, 1956. This work was supported by the U. S. Navy at the Univ. of Calif. under contract N7-ONR-29529 and is based on a thesis submitted in partial fulfillment of the requirements for the Ph.D. degree, Dept. of Elec. Eng., Univ. of Calif., 1956.

† Lockheed Aircraft Corp., Sunnyvale, Calif.

[1] H. A. Bethe, "Formal Theory of Waveguides of Arbitrary Cross Section," M.I.T. Rad. Lab. Rep. 43-26; March 16, 1943.

[2] H. A. Bethe, "Lumped Constants for Small Irises," M.I.T. Rad. Lab. Rep. 43-22; March 24, 1943.

[3] H. A. Bethe, "Theory of Side Windows in Wave Guides," M.I.T. Rad. Lab. Rep. 43-27; April 4, 1943.

Dipole Moments

The ferrite in the window will affect both the electric and magnetic dipole moments. It is assumed that the isotropic permeability of the ferrite is real and unity for microwaves, and that the dielectric constant is different from unity. The anisotropic permeability of the ferrite is a tensor and is given by expressions in the Appendix. Further, it is postulated that the dipole moment of the filled aperture can be replaced by two other dipole moments: one to account for the aperture itself and the other to account for the material in the aperture. From Bethe[4] it is known that the "equivalent" dipole moments of the empty window are given as

$$-\Pi_w = \mathfrak{M}_1 H_{0l}\bar{l} + \mathfrak{M}_2 H_{0m}\bar{m} \tag{1a}$$

$$\Phi_w = \epsilon_0 \mathcal{P}\bar{n}\cdot\overline{E}_0 \tag{1b}$$

where ϵ_0 is the electric inductive capacity of free space; $\overline{E}_0$, $\overline{H}_0$ are the fields that would exist at the center of gravity of the window if the window were replaced by a metal wall; and $\mathfrak{M}_1$, $\mathfrak{M}_2$, and $\mathcal{P}$ are the magnetic and electric polarizabilities, respectively.

Since the material in the window introduces a magnetization and a polarization, assume that the "equivalent" dipole moments of the body in the window are given as

$$\Pi_b = \mathfrak{M}_1 M_{0l}\bar{l} + \mathfrak{M}_2 M_{0m}\bar{m} \tag{2a}$$

$$\Phi_b = \mathcal{P}\bar{n}\cdot\overline{P}. \tag{2b}$$

Eqs. (2a) and (2b) are deduced by noting that, in general, the electric or magnetic dipole moment of a material is the product of its volume and the polarization or magnetization. Since the polarizabilities $\mathfrak{M}_1$, $\mathfrak{M}_2$, and $\mathcal{P}$ have the dimensions of a volume and depend upon the shape of the window, it is assumed that the volume of the material can be replaced by the polarizabilities of the window when the material is located in the window.

The total "equivalent" magnetic dipole moment of the filled aperture is the sum of (1a) and (2a); the total "equivalent" electric dipole moment of the filled aperture is the sum of (1b) and (2b). Thus, the following expressions are obtained for the total "equivalent" magnetic and electric dipole moments:

$$-\mu_0\overline{\Pi} = \mathfrak{M}_1 B_{0l}{}^{\#}\bar{l} + \mathfrak{M}_2 B_{0m}{}^{\#}\bar{m} \tag{3a}$$

$$\Phi = \mathcal{P}\bar{n}\cdot\overline{D}_0 \tag{3b}$$

where

$$B_0{}^{\#} = \mu_0(\overline{H}_0 - \overline{M}_0)$$

$$\overline{D}_0{}^{\#} = \epsilon_0 Q\overline{E}_0.$$

The quantity Q is a number greater than unity and expresses the fact that the polarization increases the magnitude of the electric dipole moment. The value of Q is determined from experiment and the quantity $\overline{H}_0 - \overline{M}_0$ is determined from the theory of the anisotropic magnetization of a ferrite. This is considered briefly in the Appendix. However, the result is that

$$B_{0l}{}^{\#} = \mu_{ll}{}^{\#}H_{0l} + \mu_{lm}{}^{\#}H_{0m}$$

$$B_{0m}{}^{\#} = \mu_{ml}{}^{\#}H_{0l} + \mu_{mm}H_{0m} \tag{4}$$

where

$$\mu_{ll}{}^{\#} = \mu_{mm}{}^{\#} = \mu_0(1 - \chi_{ll})$$

$$\mu_{lm}{}^{\#} = -\mu_{ml}{}^{\#} = -\mu_0\chi_{lm}.$$

The magnetostatic field is applied in the n direction, while the microwave field is applied in the plane normal to $\bar{n}$.

General Coupling Expressions

In this section, the expressions for the amplitudes of the normal modes coupled by a window between two waveguides is derived. Since this theory is well known, the presentation is brief.

Silver[5] gives the following expressions for the field components of freely propagating modes in waveguides of arbitrary but uniform cross section:

TE waves:

$$H_z = jH_{az}\exp(\mp j\beta_a z); \qquad H_{az} = K_a{}^2(\omega\mu)^{-1}\psi_a$$

$$\overline{E}_t = \overline{E}_{at}\exp(\mp j\beta_a z); \qquad \overline{E}_{at} = \nabla_t\psi_a \times \bar{i}_z$$

$$\overline{H}_t = \pm H_{at}\exp(\mp j\beta_a z); \qquad \overline{H}_{at} = \beta_a(\omega\mu)^{-1}\nabla_t\psi_a. \tag{5}$$

TM waves:

$$E_z = \pm jE_{az}\exp(\mp j\beta_a z); \qquad E_{az} = K_a{}^2\beta_a{}^{-1}\phi_a$$

$$\overline{E}_t = \overline{E}_{at}\exp(\mp i\beta_a z); \qquad \overline{E}_{at} = \nabla_t\phi_a$$

$$\overline{H}_t = \pm \overline{H}_{at}\exp(\mp j\beta_a z); \qquad \overline{H}_{at} = \omega\epsilon\beta_a{}^{-1}\bar{i}_z \times \nabla_t\phi_a. \tag{6}$$

Also,

$$P_{aa} = \frac{1}{2}S_a = \frac{1}{2}\int \overline{E}_{at}\times\overline{H}_{at}\cdot\bar{i}_z ds$$

$$P_{ab} = 0.$$

The functions $\overline{H}_{az}$, E_{at}, E_{az}, $\overline{H}_{at}$ are all real. Further, β_a is the phase constant; ω is the angular frequency; μ and ϵ are the magnetic and electric inductive capacities, respectively; K is the eigenvalue of $(\nabla_t{}^2 + K_a{}^2)F = 0$, where F is ψ_a or ϕ_a as the case may be; and $\omega^2\mu\epsilon = K_a{}^2 + \beta_a{}^2$. Exp $(j\omega t)$ time dependence is assumed and mks units are used throughout. The subscripts a and b in (5) and (6) designate the pair of mode indices mn and should not be confused with the transverse dimensions of rectangular waveguides.

Also needed are expressions for the fields (5) and (6) when the waveguide is shorted at an arbitrary location:

Short at $z = d$, $-\infty \leq z \leq d$:

$$H_z = 2H_{az}\exp(-j\beta_a d)\sin\beta_a(z - d)$$

$$E_z = 2jE_{az}\exp(-j\beta_a d)\cos\beta_a(z - d)$$

$$\overline{E}_t = -2j\overline{E}_{at}\exp(-j\beta_a d)\sin\beta_a(z - d)$$

$$\overline{H}_t = 2\overline{H}_{at}\exp(-j\beta_a d)\cos\beta_a(z - d). \tag{7}$$

[4] Bethe, footnote 2, see (18) and (25).

[5] S. Silver, "Microwave Antenna Theory and Design," McGraw-Hill Book Co., Inc., New York, N. Y., art. 7.3; 1949.

Short at $z=-d$, $-d\leq z\leq\infty$:

$$\begin{aligned} H_z &= -2H_{az}\exp(-j\beta_a d)\sin\beta_a(z+d)\\ E_z &= -2jE_{az}\exp(-j\beta_a d)\cos\beta_a(z+d)\\ \overline{E}_t &= 2j\overline{E}_{at}\exp(-j\beta_a d)\sin\beta_a(z+d)\\ \overline{H}_t &= -2\overline{H}_{at}\exp(-j\beta_a d)\cos\beta_a(z+d). \end{aligned} \tag{8}$$

It has been shown by Bethe[1] and by Silver[6] that the modal amplitudes of the fields set up in an infinite waveguide by a window in the wall are the following:

$$2A_aS_a = -\int_w \overline{E}_1\times\overline{H}_2^{-}\cdot\bar{n}ds \tag{9}$$

$$2B_aS_a = -\int_w \overline{E}_1\times\overline{H}_2^{+}\cdot\bar{n}ds. \tag{10}$$

The $+$ and $-$ superscripts on the field $\overline{H}_2$ indicate waves going in the direction of positive or negative z, respectively. The field $\overline{E}_1$ is the electric field set up in the guide by the window. The field $\overline{H}_2$ is a normal mode field of the waveguide when the window is absent. The surface integral is over the window, and the set of axes l, m, n are fixed in the aperture. Further, the l direction is always parallel to the long dimension of the aperture, the m direction is always parallel to its narrow dimension, and n points away from the source of excitation.

Eqs. (9) and (10) are also valid when the excited waveguide is semi-infinite and when either side-window or end-window coupling (iris coupling) is being considered. In either case, it is only necessary to obtain the field $\overline{H}_2$ in (9) and (10) from (7) or (8), rather than from (5) or (6).

The integrals in (9) and (10) have been evaluated by Bethe[7] when the window is empty. When the window is filled with a ferrite, they become

$$\begin{matrix} 2A_aS_a \\ 2B_aS_a \end{matrix} = -j\omega(\mp\mathfrak{M}_1B_{0l}{}^{\#}H_{2l}+\mathfrak{M}_2B_{0m}{}^{\#}H_{2m}+\mathcal{P}D_{0n}{}^{\#}E_{2n}). \tag{11}$$

The fields $\overline{B}_0{}^{\#}$ and $\overline{D}_0{}^{\#}$ are defined in (3) and (4). The upper signs in (11) refer to A_a; the lower signs refer to B_a. For a circular window of radius r, $\mathfrak{M}_1=\mathfrak{M}_2=(4/3)r^3$ and $\mathcal{P}=(2/3)r^3$. For apertures of other shapes, $\mathfrak{M}_1$ always corresponds to an incident magnetic field parallel to the long dimension of the aperture, while $\mathfrak{M}_2$ refers to the narrow dimension of the aperture. It should be noted that $\mathfrak{M}_1$ and $\mathfrak{M}_2$ are functions only of the shape of the window and are not to be confused with the fields 1 and 2. For a specific application, the fields $\overline{E}_2$, $\overline{H}_2$ will be defined by one of the expressions (5)–(8); the fields $\overline{E}_0$, $\overline{H}_0$ will be defined by one of the same expressions except that the mode index a is replaced by b. Eq. (11) is also valid when the waveguides are semi-infinite and for iris coupling between waveguides.

[6] *Ibid.*, art. 9.10.
[7] Bethe, footnote 2, see (51) and (55).

Coupling Through Side Windows

In this section, the general expression (11) is evaluated for two particular cases: 1) the axis of the primary guide (source of excitation) is parallel to the axis of the secondary guide (excited guide), and 2) the axis of the primary guide is perpendicular to that of the secondary guide.[8] The first device is designated as a parallel coupler,[9] and the second device as a perpendicular coupler. The set of axes fixed in the primary waveguide is denoted by ξ, η, ζ; the set of axes fixed in the secondary waveguide is denoted by x, y, z. As mentioned before the set of axes l, m, n are fixed in the aperture. The orientation of the three sets of axes is illustrated in Fig. 1. However, m and z are made parallel for the two couplers under consideration. Also, the mode index a applies to the secondary guide, and the mode index b applies to the primary guide. Case A is defined as the situation where identical rectangular waveguides are joined on their broad sides, the TE_{10} mode is propagated, and the window is centered.

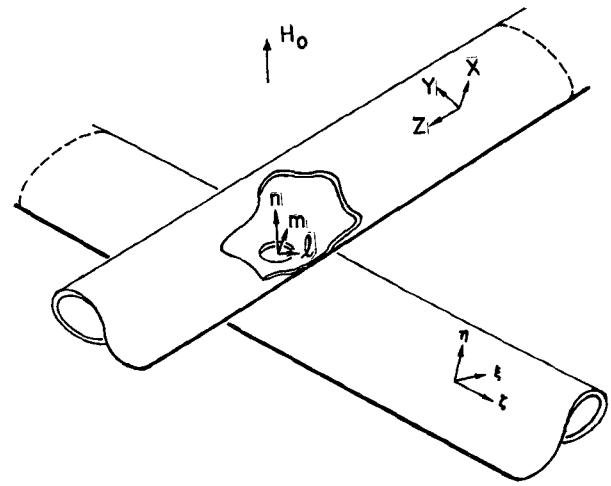

Fig. 1—Orientation of axes.

[8] Both of these waveguide configurations were considered by A. D. Berk and E. Strumwasser, "Ferrite directional couplers," PROC. IRE, vol. 44, pp. 1439–1446; October, 1956. However, their work was based on the theory of scattering by an obstacle in a waveguide. Further, they considered only ferrite cylinders extending into both waveguides with the coupling holes located at positions of circular polarization of the magnetic field. The theory presented in this paper is also applicable to these situations and is sufficiently different, it is felt, to warrant a paper on these configurations. Such a paper is nearing completion.

[9] This particular waveguide configuration was also studied by R. W. Damon, "Magnetically controlled microwave directional coupler," *J. Appl. Phys.*, vol. 26, pp. 1281–1283; October, 1955. His work is of a qualitative nature and considers a ferrite cylinder located at the position of circular polarization of the magnetic field. Furthermore, his theory is also based upon an extension of Bethe's coupling theory. However, his theory is not of a general nature but merely replaces the magnetic dipole moment of the hole by the magnetic dipole moment of the ferrite body in the hole.

It would seem that we conceived the idea of extending Bethe's coupling theory about the same time. The author originally felt that Bethe's method could be extended to treat the case of an anisotropic ferrite filling the coupling hole (Inst. of Eng. Res., Progress Rep. Ser. No. 60, Issue No. 7, Electronics Res. Lab., Univ. of Calif., Berkeley, Calif., p. 11; January 15, 1955) and later developed such a theory during the summer of 1955 (Progress Rep. Ser. No. 60, Issue No. 10, p. 9; October 15, 1955).

Parallel Coupler, Primary and Secondary Waveguides Infinite

Expressions for A_a and B_a are obtained from (11), where the fields $\overline{E}_2$, $\overline{H}_2$ are specified in (5) or (6). The fields $\overline{D}_0{}^{\#}$, $\overline{B}_0{}^{\#}$ are given in (3) and (4); the fields $\overline{E}_0$, $\overline{H}_0$ are given by (1) or (2). This results in

$$\begin{matrix}2A_aS_a\\2B_aS_a\end{matrix} = -j\omega\left[(\mp\mathfrak{M}_1H_{al}\mu_{ll}{}^{\#}+j\mathfrak{M}_2H_{az}\mu_{ml}{}^{\#})H_{bl}+j(\mp\mathfrak{M}_1H_{al}\mu_{lm}{}^{\#}+j\mathfrak{M}_2H_{az}\mu_{mm}{}^{\#})H_{bz}+\epsilon_0\mathcal{P}QE_{an}E_{bn}\right]. \quad (12)$$

It should be noted that the transverse components of the fields with the mode indices a and b have been left in the aperture coordinates, since all that was specified thus far is that m and z and ζ are parallel. However, once the orientations of the ln, $\xi\eta$, and xy axes are prescribed, one should insert the field components in their proper coordinate systems. Therefore, if (5) is used in (12), the following expression results for Case A:

$$\begin{matrix}2A_aS_a\\2B_aS_a\end{matrix} = -j\omega\left[\mp\mathfrak{M}_1\pi^2\beta^2(\omega^2\mu^2a^2)^{-1}\mu_{ll}{}^{\#}+\epsilon_0\pi^2a^{-2}Q\mathcal{P}\right]. \quad (13)$$

In (13), use has been made of the fact that $H_{al}=-H_{ax}$, $H_{bl}=-H_{b\xi}$, $E_{an}=E_{a\eta}$, and $E_{bn}=E_{b\eta}$.

If a round coupling hole of diameter d and thickness t is considered, (13) reduces to the following:

$$\begin{matrix}A_a\\B_a\end{matrix} = -j\pi d^3(3ab\lambda_g)^{-1}F_H\left[\mp\chi_{xy}+1/2(\lambda_g/\lambda_0)^2QF_EF_H{}^{-1}\right]. \quad (18)$$

Perpendicular Coupler, Primary Waveguide Semi-Infinite, Secondary Waveguide Infinite

This situation is the same as the preceding case, except that the fields H_ξ, H_ζ, and E_η are given by (7) with the mode index a replaced by b, instead of by (5) or (6). Thus, for a short at $z=d$, $-\infty\leq z\leq d$, and window at the origin:

$$\begin{matrix}A_aS_a\\B_aS_a\end{matrix} = -j\omega\exp(-j\beta_bd)\left\{-(\mp\mathfrak{M}_1H_{al}\mu_{lm}{}^{\#}+j\mathfrak{M}_2H_{az}\mu_{mm}{}^{\#})H_{b\xi}\cos\beta_bd - \left[(\pm\mathfrak{M}_1H_{al}\mu_{ll}{}^{\#}-j\mathfrak{M}_2H_{az}\mu_{ml}{}^{\#})H_{b\zeta}-j\epsilon_0\mathcal{P}QE_{an}E_{b\eta}\right]\sin\beta_bd\right\}. \quad (19)$$

$$\begin{matrix}A_a\\B_a\end{matrix} = -j\pi d^3(3ab\lambda_g)^{-1}F_H\left[\mp(1-\chi_{xx})+1/2(\lambda_g/\lambda_0)^2QF_EF_H{}^{-1}\right] \quad (14)$$

where $F_E=F_H=\exp\left\{-2\pi t\lambda_c{}^{-1}\left[1-(\lambda_c/\lambda_0)^2\right]^{1/2}\right\}$; λ_c is different for F_E and F_H,[10] since the electric and magnetic fields (although below cutoff) in the window propagate as different modes. It was assumed that the terms F_E and F_H are not affected by the presence of the material in the hole.

Perpendicular Coupler, Primary and Secondary Waveguides Infinite

Expressions for A_a and B_a are again obtained from (11), and the fields $\overline{E}_2$, $\overline{H}_2$ are specified in (5) or (6). However, the fields $\overline{B}_{0\#}$ must be made proportional to the proper fields in the primary waveguide. Thus,

$$\begin{aligned}B_{0l}{}^{\#} &= -\mu_{ll}{}^{\#}H_\zeta-\mu_{lm}{}^{\#}H_\zeta\\ B_{0m}{}^{\#} &= -\mu_{ml}{}^{\#}H_\zeta-\mu_{mm}{}^{\#}H_\zeta.\end{aligned} \quad (15)$$

[10] C. G. Montgomery, "Technique of Microwave Measurements," McGraw-Hill Book Co., Inc., New York, N. Y., p. 862; 1947.

If $\overline{B}_0{}^{\#}$ from (15) and $\overline{D}_0$ from (3) are substituted into (11) after using the proper field components from (1) or (2), the following expression results:

$$\begin{matrix}2A_aS_a\\2B_aS_a\end{matrix} = -j\omega\left[j(\pm\mathfrak{M}_1H_{b\zeta}H_{al}\mu_{ll}{}^{\#}-\mathfrak{M}_2H_{b\xi}H_{az}\mu_{mm}{}^{\#})\pm\mathfrak{M}_1H_{b\xi}H_{al}\mu_{lm}{}^{\#}+\mathfrak{M}_2H_{b\zeta}H_{az}\mu_{ml}{}^{\#}+\epsilon_0\mathcal{P}QE_{b\eta}E_{an}\right]. \quad (16)$$

With the field components in (16) given by (5), the following expression results for Case A:

$$\begin{matrix}2A_aS_a\\2B_aS_a\end{matrix} = -j\omega\left[\mp\mathfrak{M}_1\pi^2\beta^2(\omega^2\mu^2a^2)^{-1}\mu_{lm}{}^{\#}+\epsilon_0\pi^2a^{-2}\mathcal{P}Q\right]. \quad (17)$$

For a round coupling hole of diameter d, (17) simplifies to

Using the field values from (5) in (19), the following relation is obtained for Case A and $\beta_bd=q\pi$, where q is an integer:

$$A_aS_a = -B_aS_a = j\omega\mathfrak{M}_1\pi^2\beta^2(\omega^2\mu^2a^2)^{-1}\mu_{lm}{}^{\#}. \quad (20)$$

For a round coupling hole of diameter d, (20) reduces to

$$A_a = -B_a = -j2\pi d^3(3ab\lambda_g)^{-1}F_H\chi_{xy}. \quad (21)$$

Experimental Results for Side-Window Coupling

In the last section, the amplitudes of the modes coupled by the parallel and perpendicular coupler were evaluated. Here, the coupled power for Case A conditions and for a round coupling hole is calculated. The power coupled into the secondary waveguide by the window is equal to the square of A_a or B_a, since these amplitudes have been derived for unit amplitude incident fields in the primary waveguide.

The coupled power for (14) becomes

$$C_{\parallel}{}^{\pm} = C_0+10\log\left\{\left[\mp(1-C'A)+1/2(\lambda_g/\lambda_0)^2QF\,F_H{}^{-1}\right]^2+(C'B)^2\right\} \quad (22)$$

where

$$C_0 = 20 \log [\pi d^2(3ab\lambda_g)^{-1}F_H].$$

The upper and lower signs refer to the mode coupled in the same and opposite directions, respectively, as that of the incident mode. The quantities A, B, and C' are defined in the Appendix. For $d=0.1235''$, $t=0.020''$, $F_H=0.555$, and $f=9.350$ kmc, the unperturbed magnetic coupling (C_0) is -55.3 db. Thus, (22) becomes

$$C_{\parallel}^{\pm} = -55.3 + \log \{[\mp(1 - C'A) + 0.8189Q]^2 + (C'B)^2\}. \quad (23)$$

When no magnetostatic field is applied, the ferrite is isotropic, and C' vanishes. Consequently, the factor Q can be evaluated experimentally from the zero magnetostatic field expressions. The value used here in comparing theory and experiment will be an average value rather than one which gives the best agreement. Therefore, the resultant curves will not agree exactly at the zero magnetostatic field point, but this is acceptable since the interest here is in qualitative agreement.

Comparison of the theoretical expression (23) with experimental results is offered in Fig. 2 for a Ferramic A sphere. (Parameter λ_1, is proportional to the damping constant and is defined in the Appendix.) According to theory, the diagonal susceptibility is an even function of the applied magnetostatic field. Since the experimental curves for both directions of magnetostatic field were the same within the limits of experimental error, only the experimental curves for one direction of the applied magnetostatic field is presented.

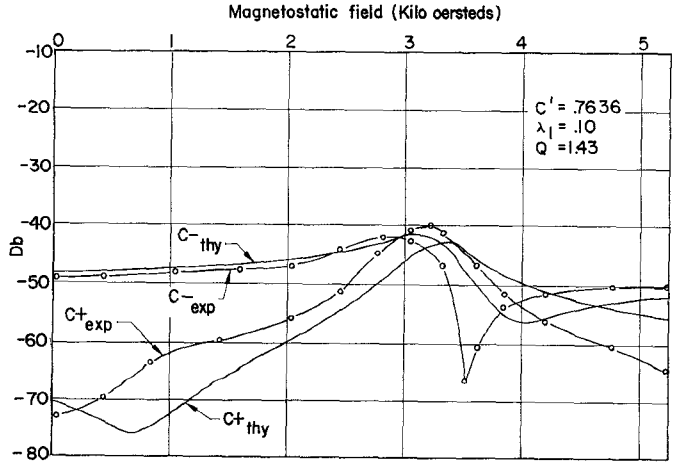

Fig. 2—Forward and reverse coupling in parallel coupler, Ferramic A sphere, both waveguides infinite.

The effect on the reverse coupling of a variation in Q is shown in Fig. 3 for a Ferramic A sphere. Note that an increase in Q increases the initial coupling slightly and also reduces the variation between the maximum values of coupling. This is correct since an increase in Q corresponds to an increase in the dielectric constant, which in turn corresponds to an increase in electric coupling.

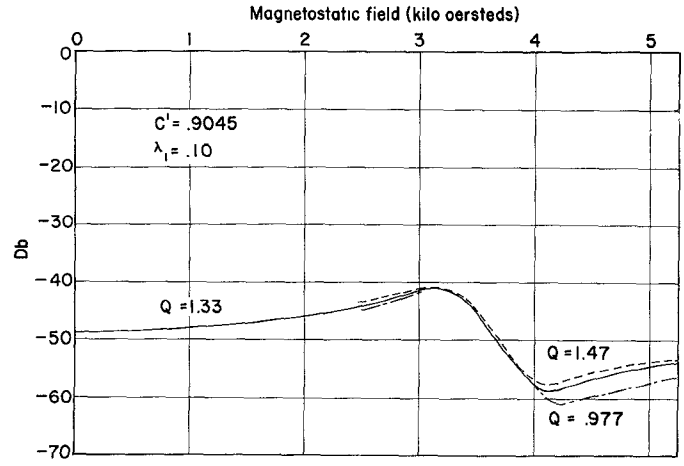

Fig. 3—Reverse coupling in parallel coupler as function of dielectric properties of Ferramic A sphere, both waveguides infinite.

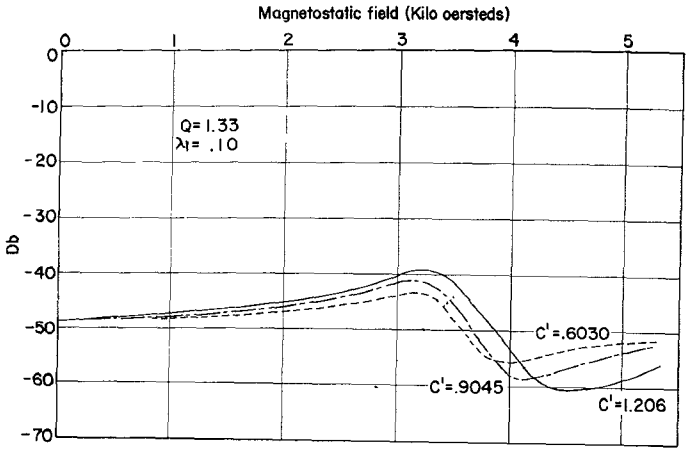

Fig. 4—Reverse coupling in parallel coupler as function of saturation magnetization of Ferramic A sphere, both waveguides infinite.

Fig. 4 shows the effect on the reverse coupling of a variation in saturation magnetization. A reduction of this parameter causes a reduction of the coupled magnetic field, thereby reducing the perturbing effect of the ferrite.

The third parameter of the ferrite studied is the damping constant. The behavior of the reverse coupling for various reduced damping constants is shown in Fig. 5. It should be remembered that the reduced damping constant is the ratio of the actual damping constant to the magnetization (saturation magnetization here). This parameter is the most critical of the three, as one would expect in a resonance-type phenomenon. Note that a reduction of the damping constant causes an increase of the perturbing effect of the ferrite.

The coupled power for (18) becomes

$$C_{\perp}^{\pm} = -49.4 + 10 \log [(\pm EF + 0.845Q)^2 + (EG)^2] \quad (24)$$

where $d=0.1495$ inch, $t=0.020$ inch, F_H-0.617, $f=9.350$ kmc, and the unperturbed coupling (C_0) is -49.4 db.

The quantities EF and EG are defined in the Appendix and are odd functions of the applied magnetostatic field. This means that a reversal of the direction of the magnetostatic field results in an interchange of the forward and reverse couplings: that is, $C^+(+)=C^-(-)$ and

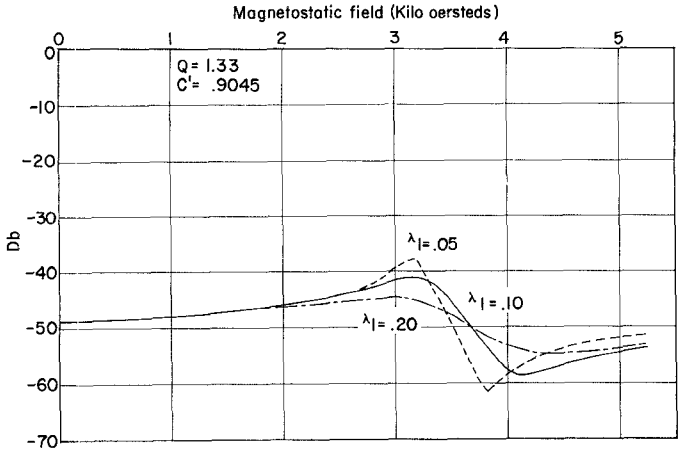

Fig. 5—Reverse coupling in parallel coupler as function of reduced damping constant of Ferramic A sphere, both waveguides infinite.

$C^+(-)=C^-(+)$, where, for instance, $C^+(-)$ indicates the forward coupling for negative values of the applied magnetostatic field. Comparison of theory and experiment for positive values of the applied magnetostatic field is illustrated in Fig. 6 for a Ferramic A sphere. The agreement between theory and experiment is acceptable, although it is felt that better quantitative agreement can be obtained by choosing a smaller value for the reduced damping constant.

The coupled power for (21) becomes

$$C_{\perp}^{\pm} = -43.4 + 10 \log [E^2(F^2 + G^2)] \qquad (25)$$

where C_0 is 6 db larger because of the short in the primary waveguide. The constants of the window are the same as for (24). Since the short in the primary waveguide is located so as to annul the electric coupling, there is no coupling into the secondary waveguide until the ferrite becomes anisotropic. Note in Fig. 7, for Ferroxcube 4-A, that a small value of the magnetostatic field is sufficient to increase the coupling to the value it would normally be when only the electric field couples. Agreement is quite satisfactory except for small values of applied magnetostatic field. One sees very clearly that the theoretical curve predicts too large a coupling initially. This is probably caused by the fact that the actual magnetization has been replaced by the saturation magnetization. The agreement at resonance could also be improved by using a smaller reduced damping constant.

Although the theory derived is valid only when the coupling aperture is completely filled with a material, it is of interest to examine experimentally the effect on

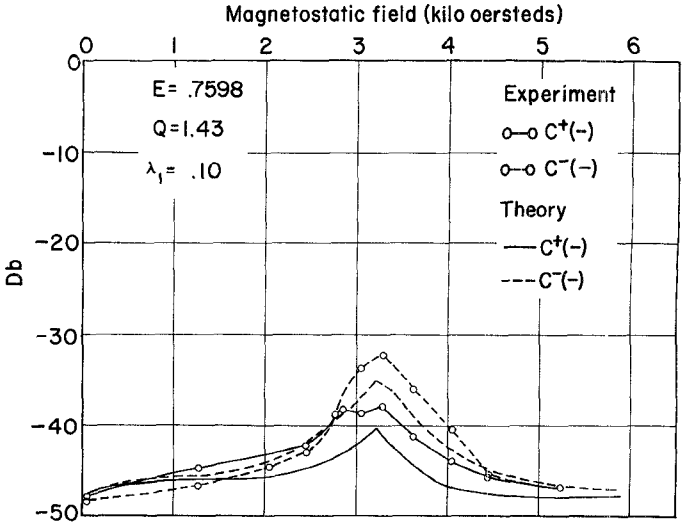

Fig. 6—Forward and reverse coupling in perpendicular coupler, Ferramic A sphere, both waveguides infinite.

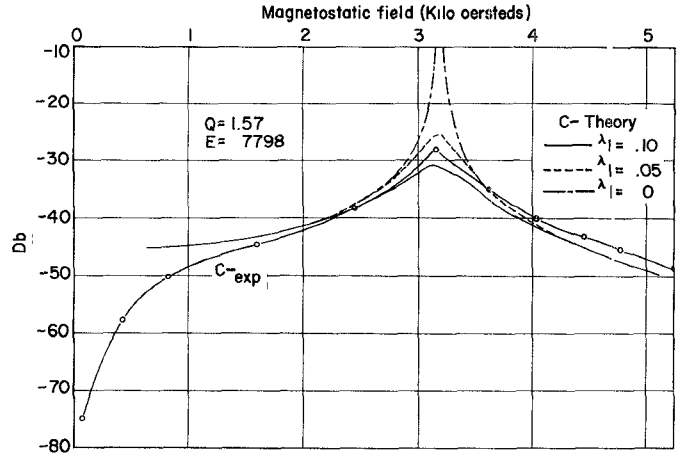

Fig. 7—Reverse coupling in perpendicular coupler as function of reduced camping constant of Ferroxcube 4-A sphere, primary waveguide semi-infinite, secondary waveguide infinite.

the magnetic coupling of partially filling the aperture with a ferrite. In this case, shorts were used to annul the electric coupling. However, the electric coupling could also be excluded by properly choosing the location of the window. For comparison purposes, the magnetic coupling curves for a spherical, a rectangular, and a disk-shaped Ferroxcube 4-A sample are shown in Fig. 8. The spherical and disk-shaped samples were placed in a round aperture; the rectangular sample was placed in a rectangular aperture with the long dimension parallel to the axis of the primary waveguide. These were all obtained with the perpendicular coupler and for Case A conditions. The curves for the rectangular and disk-shaped samples are very similar. However, the curve for the spherical sample has a much larger amplitude at resonance than either of the other curves, and its resonance also occurs for a much smaller value of applied magnetostatic field.

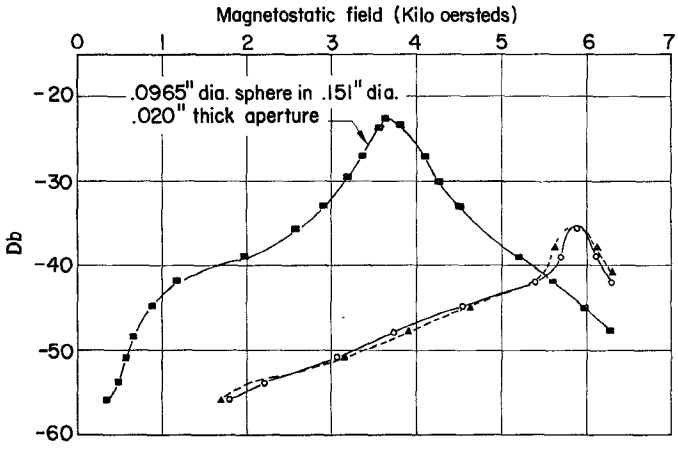

Fig. 8—Effect on magnetic coupling in perpendicular coupler by partially filling aperture with various shaped Ferroxcube 4-A samples. ■ 0.0965 inch dia. sphere in 0.151 inch dia., 0.020 inch thick aperture. ▲ 0.250 inch×0.075 inch×0.020 inch thick sample in aperture of same size and 0.010 inch thick. ○ 0.100 inch dia., 0.021 inch thick disk in 0.151 inch dia., 0.020 inch thick aperture.

Conclusion

The theory presented is satisfactory for small samples, although the sample sizes used here are near the upper size limit for these materials. For materials with smaller losses, it would be necessary to use even smaller sample sizes in order to avoid dimensional effects.

The theory of the magnetization of the ferrite is the weak link in this coupling theory. Consequently, any effort to apply this coupling theory to larger samples would require a proper modification of the magnetization expressions. It is felt that the dimensional effects in the sample enter in two ways. The first occurs because of the inhomogeneity in magnetization and can be accounted for by properly choosing the constants of the ferrite. In other words, we can choose values for the constants in such a manner as to obtain good agreement between theory and experiment but these values will not necessarily be the true constants of the material. The other effect occurs when the sample becomes electrically large and acts as a resonator. The present coupling theory does not account for this.

Appendix

Tensor Magnetization of a Ferrite

The purpose here is to evaluate the susceptibilities defined in (4). These susceptibilities result when a ferrite is made anisotropic by the application of a magnetostatic field in the n direction. Although this has been done by several authors,[11,12] part of the work is repeated here for continuity. The form followed is that given by Beljers.[11]

The fundamental equation for the magnetization, $\overline{M}$, is the following:

$$\dot{\overline{M}}\gamma^{-1} = \overline{M} \times \overline{B} - \lambda(\overline{B} - \overline{B}\cdot\overline{M}M^{-2}\overline{M}) \qquad (26)$$

where $\gamma = -ge/2m$ (the magnetomechanical ratio, a negative quantity for an electron); e and m are the electron charge and mass, respectively; g is the spectroscopic splitting factor; λ is a damping constant; and $\overline{B} = \mu_0(\overline{H} + \overline{M})$. The damping constant can be introduced in different manners, but the two commonly used forms both give identical results for the order of approximation used here.[13]

For the problem under consideration, the following is chosen:

$$H_l = h_l - (N_l - 1/3)M_l$$
$$H_m = h_m - (N_m - 1/3)M_m$$
$$H_n = H - (N_n - 1/3)M$$

where the N_i's are the demagetizing factors, the quantities h_l and h_m are the applied microwave magnetic fields, and H is the applied magnetostatic field.

Consistent with the usual assumption, the microwave magnetizations are as follows:

$$M_l = \gamma ML^{-1}[h_l\{\mu_0^2\gamma(1+\lambda_1^2)[H + M(N_m - N_n)] - j\omega\mu_0\lambda_1\} - j\omega\mu_0 h_m]$$
$$M_m = \gamma ML^{-1}[h_m\{\mu_0^2\gamma(1+\lambda_1^2)[H + M(N_l - N_n)] - j\omega\mu_0\lambda_1\} + j\omega\mu_0 h_l] \qquad (27)$$

where

$$L = -\omega^2 + \mu_0^2\gamma^2(1+\lambda_1^2)[H + M(N_l - N_m] \cdot [H + M(N_n - N_m)] - 2j\omega\mu_0\gamma\lambda_1 H - j\omega\mu_0\gamma\lambda_1 M(N_l - N_m - 2N_n),$$

$\lambda_1 = \lambda/M$ is a reduced damping constant, and M is the saturation magnetization in the n direction. When the ferrite sample is spherical, the magnetizations simplify considerably to the following:

$$M_l = \chi_{ll}h_l + \chi_{lm}h_m$$
$$M_m = \chi_{ml}h_l + \chi_{mm}h_m \qquad (28)$$

where

$$\chi_{ll} = \chi_{llr} + j\chi_{lli}$$
$$\chi_{lm} = \chi_{lmr} + j\chi_{lmi}.$$

For computational purposes, the following substitutions are made:

$$\gamma' = -\gamma$$
$$x = \mu_0\gamma' H\omega^{-1}(1+\lambda_1^2)^{1/2}. \qquad (29)$$

[11] H. G. Beljers, "Measurements on gyromagnetic resonance of a ferrite using cavity resonators," *Physica*, vol. 14, pp. 629–641; February, 1949.

[12] C. L. Hogan, "The microwave gyrator," *Bell Sys. Tech. J.*, vol. 31, pp. 1–31; January, 1952.

[13] We introduce our damping constant according to Landau and Lifschitz (see Beljers, *op. cit.*).

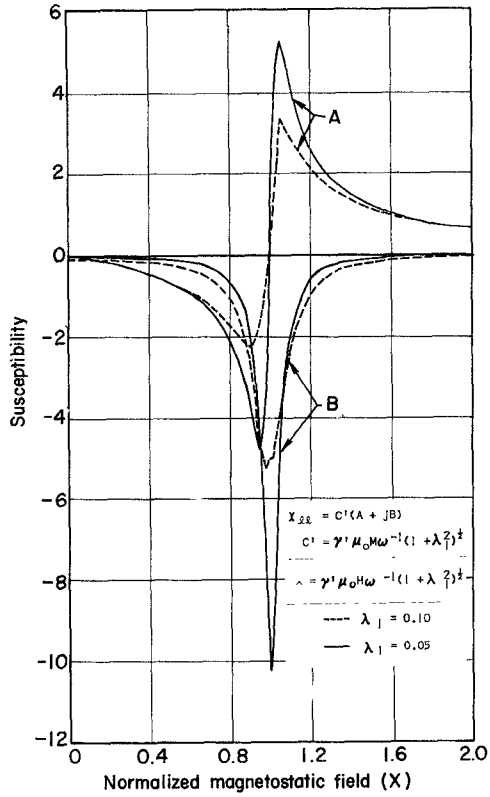

Fig. 9—Diagonal susceptibility of small ferrite sphere as function of normalized applied magnetostatic field.

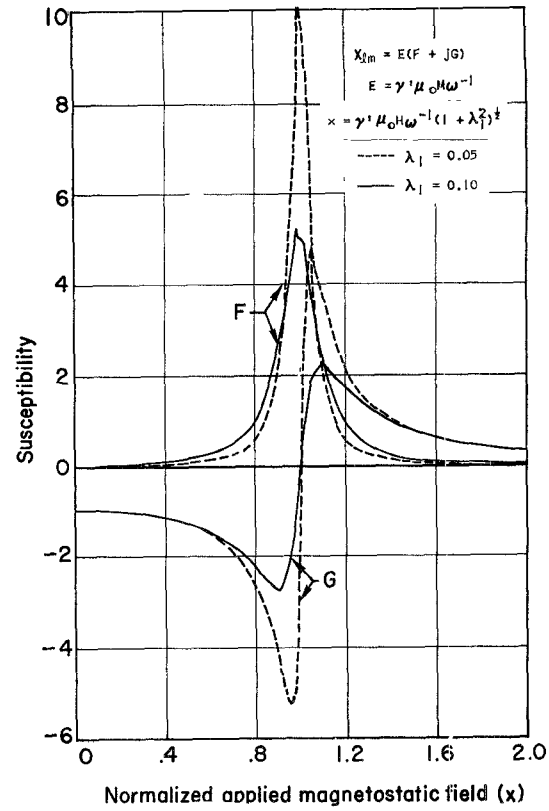

Fig 10—Nondiagonal susceptibility of small ferrite sphere as function of normalized applied magnetostatic field.

Thus, the components of the susceptibilities become

$$\begin{aligned} \chi_{llr} &= C'A \\ \chi_{lli} &= C'B \\ \chi_{lmr} &= EF \\ \chi_{lmi} &= EG \end{aligned} \tag{30}$$

where

$$\begin{aligned} C' &= \gamma'\mu_0 M\omega^{-1}(1+\lambda_1^2)^{1/2} \\ A &= a/b \\ B &= -a'/b \\ E &= \gamma'\mu_0 M\omega^{-1} \\ F &= c/b \\ G &= -c'/b \\ a &= x\{x^2 - [1 - 2\lambda_1^2(1+\lambda_1^2)^{-1}]\} \\ a' &= \lambda_1(x^2+1)(1+\lambda_1^2)^{-1/2} \\ c' &= 1 - x^2 \\ c &= 2\lambda_1 x(1+\lambda_1^2)^{-1/2} \\ b &= x^4 - 2x^2[1 - 2\lambda_1^2(1+\lambda_1^2)^{-1}] + 1. \end{aligned}$$

Note also that $\chi_{mm} = \chi_{ll}$, and $\chi_{lm} = -\chi_{ml}$.

In most ferrite work the susceptibilities are defined so that

$$\begin{aligned} M_l &= \chi h_l - jKh_m \\ M_m &= jKh_l + \chi h_m \end{aligned} \tag{31}$$

where

$$\begin{aligned} \chi &= \chi' - j\chi'' \\ K &= K' - jK''. \end{aligned}$$

Using this notation,

$$\begin{aligned} \chi' &= C'A \\ \chi'' &= -C'B \\ K' &= -EG \\ K'' &= -EF. \end{aligned} \tag{32}$$

For the simple case of no damping, the imaginary parts of both χ and K vanish. Eq. (33) then reduces to the one that is characteristic of a gyrotropic medium.

In order to understand better the behavior of the permeability of the ferrite when it is anisotropic, several families of curves of χ_{ll} and χ_{lm} are plotted as a function of x, with M and λ_1 as parameters; Fig. 9 is a plot of χ_{ll} vs x for $\lambda_1 = 0.05$ and $\lambda_1 = 0.10$. Similarly, Fig. 10 is a plot of χ_{lm} vs x for $\lambda_1 = 0.05$ and $\lambda_1 = 0.10$. In both figures, the coefficients C' and E were set equal to unity. It should also be noted that χ_{ll} is an even function of the applied magnetostatic field, whereas χ_{lm} is an odd function of the applied magnetostatic field.

ACKNOWLEDGMENT

I would like to thank Dr. D. J. Angelakos for his aid with the theoretical aspects of this work and Seymon Hersh for his help with the manuscript.